GSA Data Repository 2020111

Matchan, E.L., Phillips, D., Jourdan, F., and Oostingh, K., 2020, Early human occupation of southeastern Australia: New insights from 40Ar/39Ar dating of young volcanoes: Geology, v. 48, https://doi.org/10.1130/G47166.1

Data Repository Item: Material, Methods and Analytical Results

SAMPLE COLLECTION

The NVP18 basalt sample was collected from the Tyrendarra Quarry, Princes Hwy Tyrendarra (Fig 1; coordinates: 38°13.97' S, 141°46.25'E WGS84). A fresh, well-crystallised section through the Tyrendarra lava flow is exposed in the western wall of the quarry at approximately 2 m depth from surface, and it is from this section that a ~1 kg block of basalt (NVP18) was collected using a sledgehammer.

The VIC25 lava bomb, measuring approximately 15 cm in length, was collected *in situ* from the south-western wall of the Tower Hill maar in a ~30 m-thick section of phreatomagmatic deposits exposed by historical quarrying activity (CRB Quarry) at the entrance of what is now the Tower Hill Wildlife Reserve, approximately 12 km northwest of Warrnambool (Fig. 1; coordinates: 38°19.61' S, 142°22.10'E).

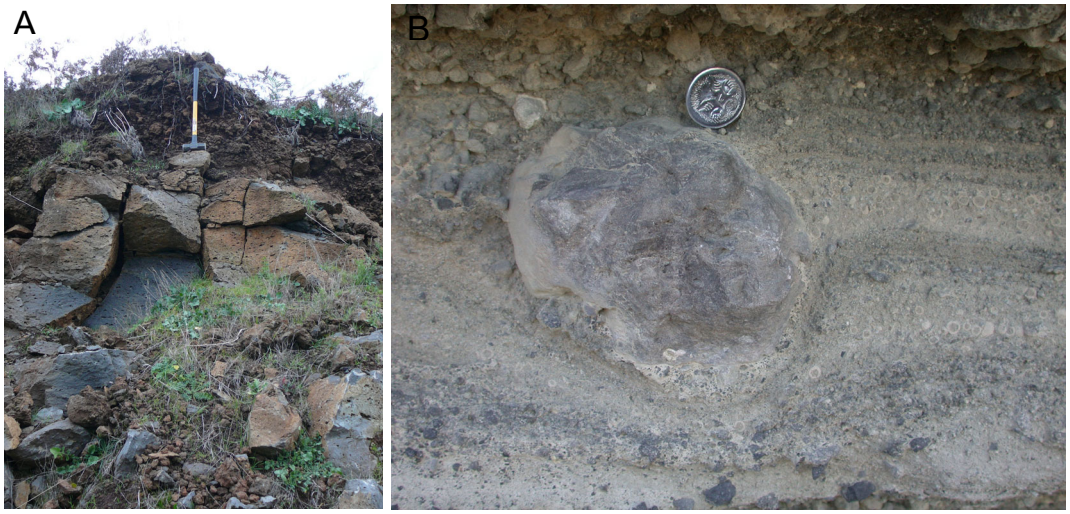

Figure DR1 A. Section of Tyrendarra basalt from which NVP18 was collected. Sledgehammer is approximately 1 m long. **B.** *In situ* lava bomb in the exposed Tower Hill phreatomagmatic sequence from which VIC25 was collected. The bomb penetrates beds of ash (pale grey) and fine scoria (dark grey), with some ash layers exhibiting accretionary lapilli. Coin is approximately 2 cm in diameter.

PETROGRAPHY

NVP18

Small phenocrysts of plagioclase (laths ≤ 0.8 mm), olivine and clinopyroxene are set in a coarsely crystalline groundmass dominated by plagioclase, clinopyroxene, olivine and magnetite (Fig. DR2a,b). The average olivine phenocryst size is 0.4 mm and clinopyroxene phenocrysts are smaller (typically ca. 0.2 mm) and less abundant. Abundant apatite needles are present in interstitial pools of feldspar. A minor amount of glass (<1% by volume) is present. Small vesicles (≤ 0.5 mm) comprise ~5% by volume.

VIC25

Microphenocrysts of clinopyroxene (≤ 0.1 mm) and olivine occur in a fine-grained groundmass dominated by plagioclase, clinopyroxene, olivine, opaques (magnetite?), apatite, and glass (~10% glass by volume; Fig. DR2c,d).

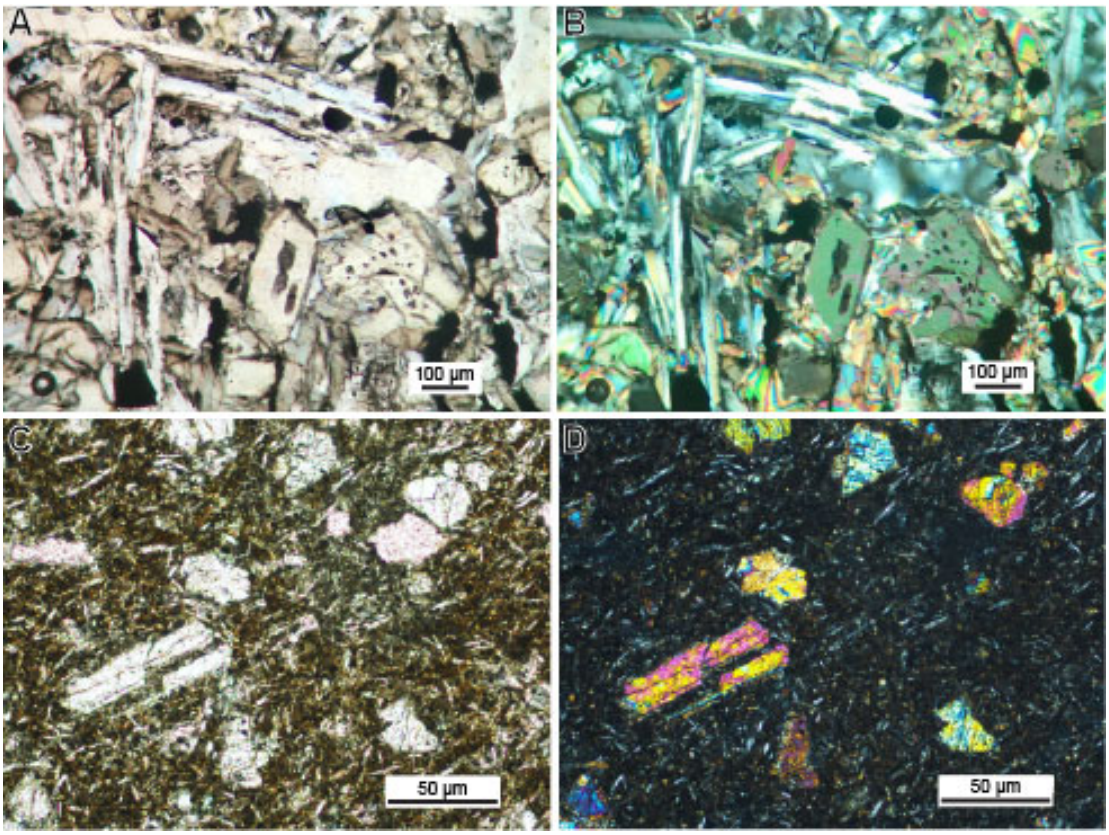

Figure DR2 A. Photomicrograph of sample NVP18 (plane polarised light). **B.** NVP18 (cross-polarised light). **C.** VIC25 (plane polarised light). **D.** VIC25 (cross-polarised light).

ANALYTICAL METHODS

NVP18

Sample preparation and analytical procedures followed those described in Matchan and Phillips (2014). Approximately 1 kg of sample was crushed to 2 cm sized chips using a jaw crusher. Individual chips were then screened for alteration and large vesicles, with acceptable chips crushed manually using a steel piston crusher. Crushed fragments were washed of dust and sieved to a 180–250 μm grain size (after Ozawa et al., 2006).

Following purification of whole rock groundmass material by magnetic separation, approximately 300 mg of groundmass material was hand-picked under a binocular microscope. Grains were treated with 5% HNO_3 for 10 min in an ultrasonic bath, followed by 2% HF for 1 min, followed by deionised water for 10 min. The sample was then loaded into an aluminium foil packet, placed in a quartz tube (UM#54), and bracketed by packets containing the flux monitor standard Alder Creek Rhyolite (ACR) sanidine. Can UM#54 was irradiated for 30 min in the Cadmium-Lined In-Core Irradiation Tube (CLICIT) facility of the Oregon State University TRIGA reactor, USA.

Individual aliquots measuring approximately 100 mg were loaded as double- to triple-grain layers into a custom-made circular copper sample holder containing four parallel slots, measuring 6 mm wide, 25- 30 mm long and 3 mm deep. The holder was covered with a ZnS glass disc and loaded into the sample chamber of a gas-handling system connected to a multi-collector Thermofisher ARGUSVI mass spectrometer in the Ar-Ar Laboratory, University of Melbourne. As described in detail by Phillips and Matchan (2013), the ARGUSVI detector array comprises 5 Faraday detectors and a CDD (compact discrete dynode) electron multiplier, allowing simultaneous collection of all 5 argon isotopes (^{36}Ar was measured on the CDD).

The extraction line and contained samples were baked for at least 12 hours at ~120°C. Once acceptable (UHV) background levels were achieved, each aliquot was heated with a Photon Machines Fusions 10.6 CO_2 laser to remove the majority of loosely-bound argon; this was achieved using the 6 mm homogenised beam focused to a narrow intense energy band perpendicular to the sample slot, operated step-wise between 1 and 2% laser power. For step-heating experiments, aliquots were heated incrementally over a range of 4–14% laser power (0.95–2.90 W). Line blanks were measured after every second or third sample analysis and were typically <1-3 fA for ^{40}Ar, compared to ≥150 fA for typical sample analyses (see Table DR1). Mass discrimination and detector bias were characterised via

automated analyses of air pipette aliquots prior to the first analysis, assuming an atmospheric $^{40}Ar/^{36}Ar$ ratio of 298.56 ± 0.31 (Lee et al., 2006).

Due to the short irradiation time it was not feasible to include Ca/K/Cl salts/glasses in the same package. Therefore, correction factors determined for K-glass and Ca-salts contained in another recent package irradiated in the CLICIT facility (UM#52) were used: $(^{39}Ar/^{37}Ar)_{Ca}$ = (6.5075 ± 0.0033) × 10^{-4}; $(^{36}Ar/^{37}Ar)_{Ca}$ =(2.7703 ± 0.0017) × 10^{-4}; $(^{40}Ar/^{39}Ar)_{K}$ = (5.88 ± 0.18) × 10^{-4}; and $(^{38}Ar/^{39}Ar)_{K}$ = (1.20540 ± 0.00072) x 10^{-2}. The J-value for sample NVP18 (0.000131244 ± 0.000000084; 0.06% 1σ) was calculated by averaging the mean $^{40}Ar^*/^{39}Ar$ ratios from fusion analyses conducted on several aliquots (three grains per aliquot) of bracketing ACR sanidine standards.

VIC25

Sample preparation and analytical procedures followed those described in Oostingh et al. (2017). Approximately 1 kg of sample was crushed in a hydraulic press to cm-scale chips, and the freshest chips were further crushed in a Tungsten-Carbide ring mill. Crushed material was then sieved to a 355–500 μm grain size and washed of dust. Approximately 300 mg of groundmass was hand-picked using a binocular stereomicroscope. Grains were treated with methanol and diluted HF (2N) for 5 min to remove any glass, followed by duplicate washes with deionised water. The sample was then loaded into an aluminium disc wrapped in aluminium foil and stacked into a quartz tube along with other sample discs and the flux monitor Fish Canyon Tuff sanidine for which an age of 28.126 ± 0.019 Ma (Phillips et al., 2017) was assumed. The vial was irradiated for 20 min in the CLICIT facility of the Oregon State University TRIGA reactor.

$^{40}Ar/^{39}Ar$ step-heating analyses were performed using the multi-collector Thermofisher ARGUSVI mass spectrometer at the West Australian Argon Isotope Facility, Curtin University, Perth. Two aliquots of irradiated sample, each weighing approximately 100 mg, were placed as a single layer in a custom-made high-grade aluminium sample disk, and loaded into the sample chamber connected to a custom-built, extra low volume (240 cm^3), stainless steel gas extraction line. The sample and extraction line were baked at 1200 C for approximately 12 h. Each aliquot was step-heated with a 100 W Photon Machines Fusions 10.6 CO_2 laser using a homogenized 4 mm beam operated between 3 and 40% laser power (maximum power of 55 W), whereas standards were fused in a single step. During each heating step, the beam was continually jogged over the sample for

approximately 1 min. The resulting gas was purified using a polycold electrical cryocooler, a liquid nitrogen condensation trap, a SAES GP50 getter operating at 4508C, a AP10 SAES getter operating at 4508C and a AP10 SAES getter operating at room temperature. As for NVP18, measurement was performed in multicollector mode with ^{37}Ar, ^{38}Ar, ^{39}Ar, and ^{40}Ar analysed on four Faraday detectors (10^{12} Ω resistors on mass 40, 38, and 37 and 10^{13} Ω on mass 39) and ^{36}Ar analysed on the CDD.

Argon isotope results are corrected for system blanks, mass discrimination, radioactive decay and reactor-induced interference reactions. System blanks were measured every fourth sample experiment. Mass discrimination was closely monitored via an automated air pipette system before and after each step-heating experiment assuming the Lee et al. (2006) atmospheric $^{40}Ar/^{36}Ar$ ratio. The J-value for all specific levels in the irradiation vial was calculated by averaging the mean ($^{40}Ar^*/^{39}Ar$) ratios from total fusion analysis of four single-grain aliquots of FC sanidine bracketing the sample. The J-value for VIC25 was 0.00009793 ± 0.00000031 (0.32%). The following correction factors obtained via prolonged irradiation of K-Ca-Cl glass/salts in the CLICIT facility of the Oregon State TRIGA reactor were applied to the data: $(^{39}Ar/^{37}Ar)_{Ca} = (7.60 \pm 0.09) \times 10^{-4}$; $(^{36}Ar/^{37}Ar)_{Ca} = (2.70 \pm 0.02) \times 10^{-4}$; $(^{40}Ar/^{39}Ar)_K = (7.30 \pm 0.90) \times 10^{-4}$; and $(^{38}Ar/^{39}Ar)_K = (1.24 \pm 0.004) \times 10^{-2}$ (Jourdan and Renne, 2007).

Age Calculations

$^{40}Ar/^{39}Ar$ ages for NVP18 and VIC25 were calculated relative to an age of 1.18144 Ma ± 0.00068 Ma (2σ) for ACR sanidine (Phillips et al. 2017), and 28.126 Ma + 0.019 Ma for FCT sanidine (Phillips et al. 2017), respectively, using the decay constants of Steiger and Jäger (1977). Calculated uncertainties associated with plateau and inverse isochron ages include uncertainties in the J-value, but exclude errors associated with the age of the flux monitor and the decay constant. Unless otherwise stated, uncertainties are reported at the 2σ level (see Ludwig, 2012). Plateau ages are defined as including ≥50% of the total ^{39}Ar, from at least 3 contiguous steps, with $^{40}Ar^*/^{39}Ar$ ratios within error of the mean at the 95% confidence level. Argon isotopic results for NVP18 and VIC25 are reported Tables DR1 and DR2, respectively. Step-heating spectra and isochron plots (Figs. 3, DR2, and DR3) were generated using ISOPLOT/Ex v.3.75 (Ludwig, 2012) and ArArCALC (Koppers, 2002) for NVP18 and VIC25, respectively. A summary of inverse isochron results for each aliquot, plateau age results and total gas ages, is provided in Table DR3.

For both samples alike, composite inverse isochrons were generated by pooling concordant data from all aliquots, selecting data from consecutive heating steps only. Anomalous intermediate steps V18-2c and VIC25-B-5M7646 were excluded from the composite inverse isochron calculations of NVP18 and VIC25, respectively. NVP18 yielded a composite inverse isochron age of 36.9 ± 3.1 ka (95% CI; MSWD = 1.7, p = 0.02, n = 24) and a corresponding initial argon value ($(^{40}Ar/^{36}Ar)_i$) of 297.9 ± 1.5 (95% CI), with the isochron data representing 85% of the total ^{39}Ar released across the four aliquots VIC25 yielded a composite inverse isochron age of 36.8 ± 3.8 ka (2σ; MSWD = 1.04, p = 0.41, n = 22) and a corresponding $(^{40}Ar/^{36}Ar)_i$ value of 301 ± 1.8 (2σ), with the included steps representing 77% of the total ^{39}Ar released across the two aliquots (Fig DR3c).

Tables DR1–DR3. Ar-Ar analytical data set and age results summary

2020111_Tables DR1-DR3.xlsx

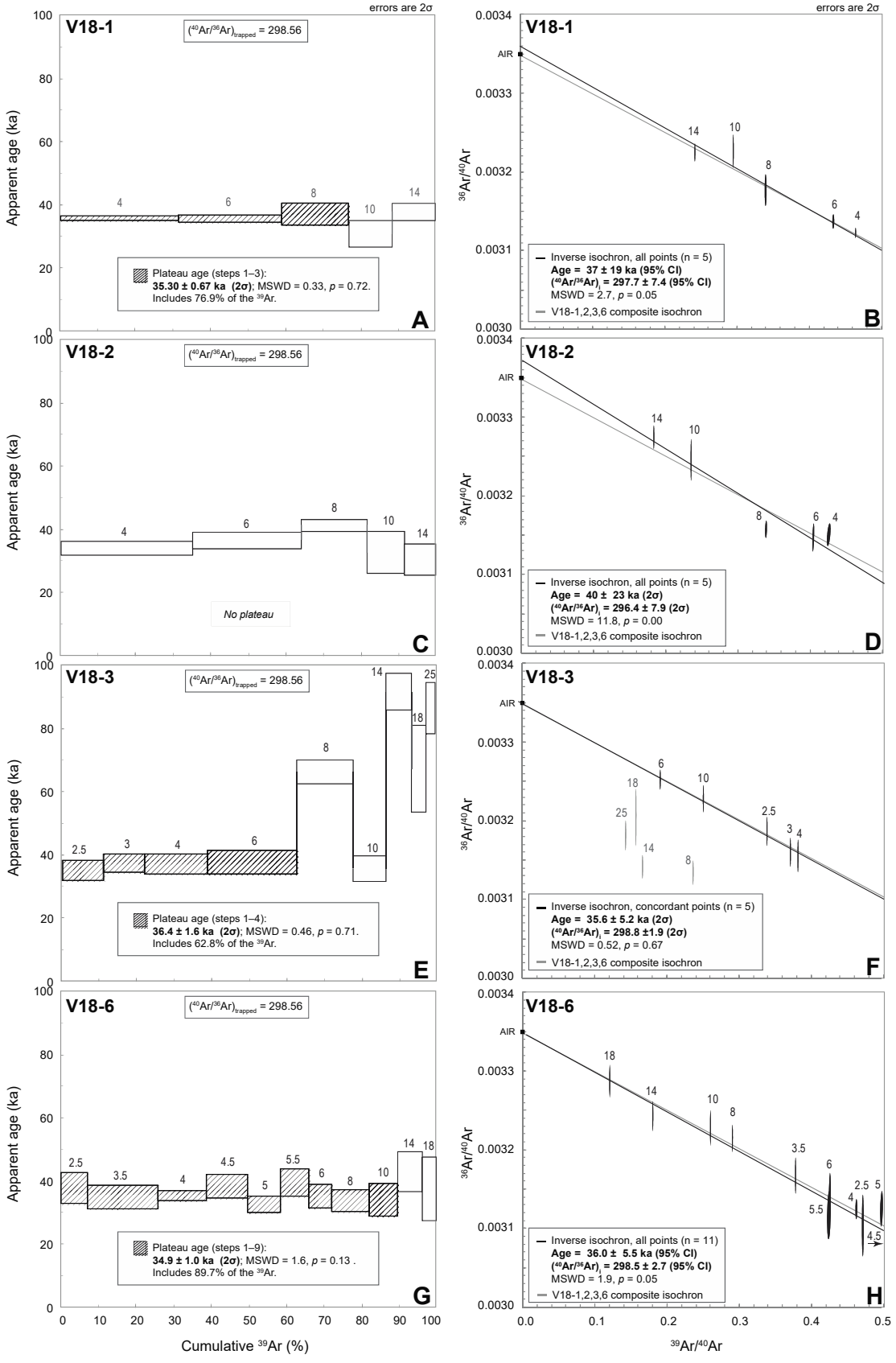

143

144 **Figure DR2. A–G.** Individual $^{40}Ar/^{39}Ar$ 'model' age spectra ($(^{40}Ar/^{36}Ar)_{trapped}$ = 298.56) and inverse isochron
145 diagrams for individual aliquots of basalt groundmass sample NVP18 (Tyrendarra flow). Data are annotated

with laser power (%). Data excluded form inverse isochrons are in grey. **I.** Composite inverse isochron for concordant points from all aliquots. Data outlined in black are included in the composite inverse isochron.

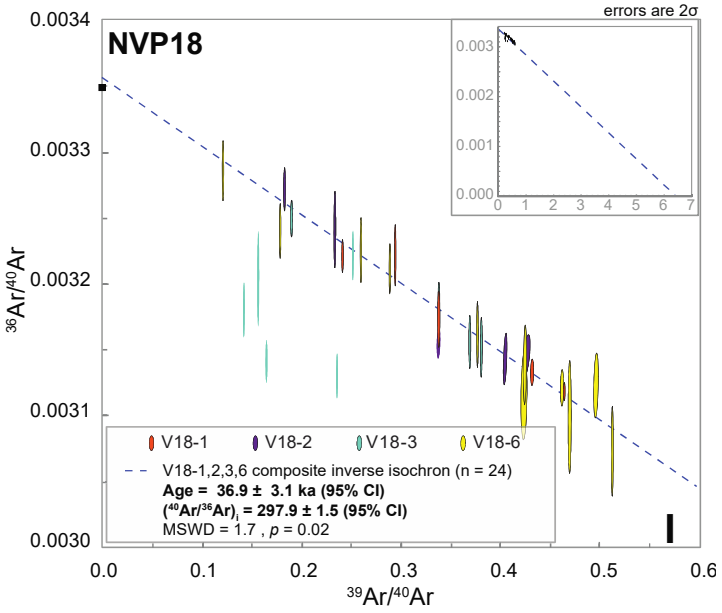

Figure DR2 cont.

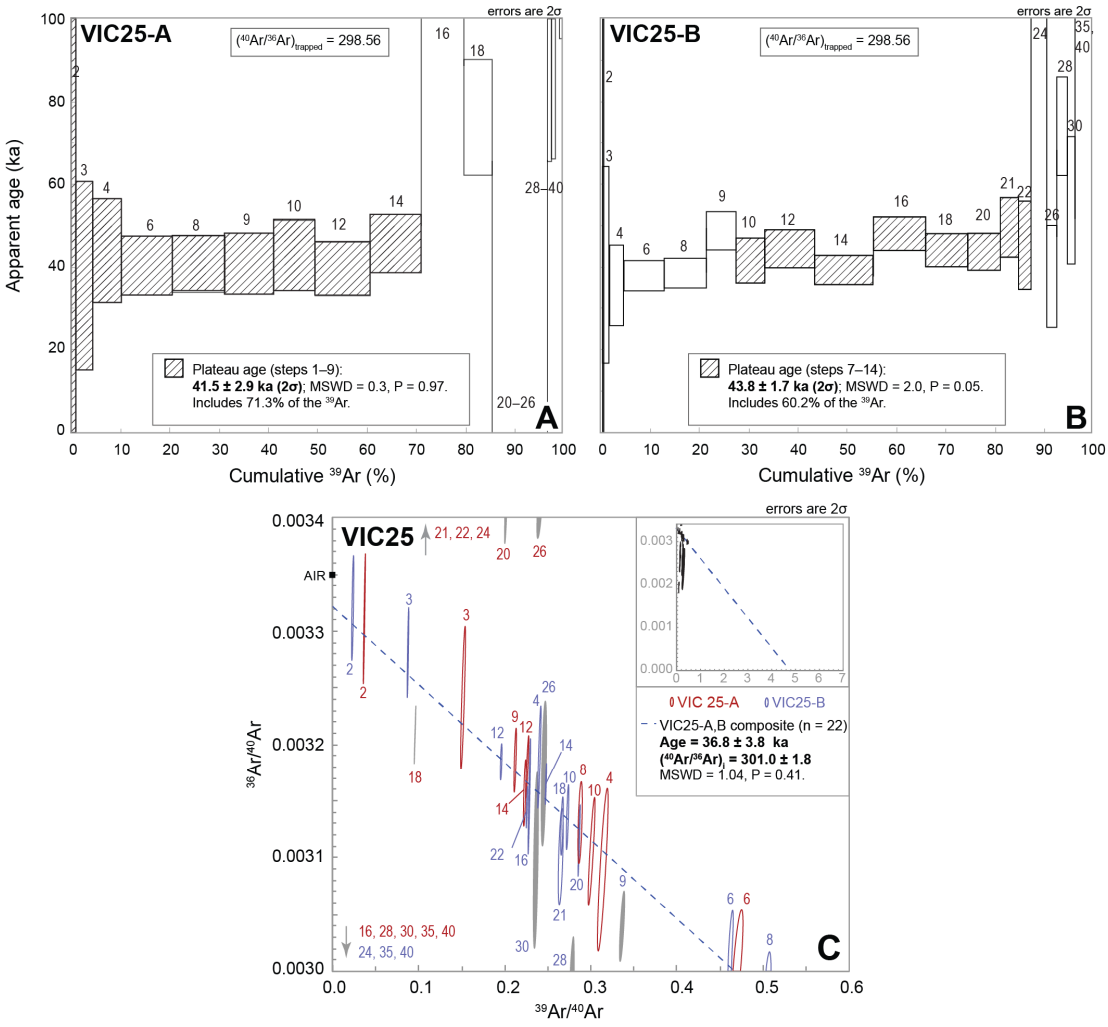

Figure DR3. **A–B.** Individual $^{40}Ar/^{39}Ar$ 'model' age spectra ($(^{40}Ar/^{36}Ar)_{trapped}$ = 298.56) for aliquots of basalt groundmass sample VIC25 (Tower Hill lava bomb groundmass). Data are annotated with laser power (%). **C.** Composite inverse isochron diagram for VIC25-A and VIC25-B. Data are annotated with laser power (%).

REFERENCES

Jourdan, F., Renne, P., 2007. Age calibration of the Fish Canyon sanidine $^{40}Ar/^{39}Ar$ dating standard using primary K-Ar standards. Geochimica et Cosmochimica Acta, v. 71, p. 387–402.

Koppers, A.A.P., 2002. ArArCALC-software for $^{40}Ar/^{39}Ar$ age calculations. Computers & Geosciences, v. 28, p. 605–619.

Lee, J.-Y., Marti, K., Severinghaus, J. P., Kawamura, K., Yoo, H.-S., Lee, J. B., and Kim, J. S., 2006, A redetermination of the isotopic abundances of atmospheric Ar: Geochimica et Cosmochimica Acta, v. 70, p. 4507-4512.

Ludwig, K. R., 2012, User's Manual for Isoplot 3.75. A Geochronological Toolkit for Microsoft Excel: Spec. Publ. No. 5, Berkeley Geochronology Center, Berkeley, California, p. 75 pp.

Matchan, E. L., and Phillips, D., 2014, High precision multi-collector 40Ar/39Ar dating of young basalts: Mount Rouse volcano (SE Australia) revisited: Quaternary Geochronology, v. 22, p. 57-64.

Oostingh, K.F., Jourdan, F., Matchan, E.L., and Phillips, D., 2017. $^{40}Ar/^{39}Ar$ geochronology reveals rapid change from plume-assisted to stress-dependent volcanism in the Newer Volcanic Province, SE Australia. Geochemistry, Geophysics, Geosystems, doi:10.1002/2016GC006601.

Ozawa, A., Tagami, T., and Kamata, H., 2006, Argon isotopic composition of some Hawaiian historical lavas: Chemical Geology, v. 226, no. 1-2, p. 66-72.

Phillips, D., and Matchan, E. L., 2013, Ultra-high precision $^{40}Ar/^{39}Ar$ ages for Fish Canyon Tuff and Alder Creek Rhyolite sanidine: new dating standards required?: Geochimica et Cosmochimica Acta, v. 121, p. 229-239.

Phillips, D., Matchan, E.L., Honda, M., and Kuiper, K.F., 2017. Astronomical calibration of $^{40}Ar/^{39}Ar$ reference minerals using high-precision, multi-collector (ARGUSVI) mass spectrometry. Geochimica et Cosmochimica Acta, v. 196, p. 351–369.

183 Steiger, R. H., and Jäger, E., 1977, Subcommission on geochronology: Convention on the
184 use of decay constants in geo- and cosmochronology: Earth and Planetary Science
185 Letters, v. 36, p. 359-362.